RESEARCH ARTICLE

DRUG DEVELOPMENT RESEARCH WILEY

Tanshinol alleviates ulcerative colitis by promoting the expression of VLDLR

Huanhuan Zhu[1] | Shaopeng Tong[2] | Yan Cui[3] | Xiaodong Wang[4] |
Minying Wang[1]

[1]Department of Anorectal Surgery, Wuxi
Traditional Chinese Medicine Hospital, Wuxi,
PR China

[2]Endoscopic Center, Wuxi YEBO Proctology
Hospital of Traditional Chinese Medicine,
Wuxi, PR China

[3]Department of Infection Control, Wuxi
Traditional Chinese Medicine Hospital, Wuxi,
PR China

[4]Department of Traditional Chinese Medicine,
Wuxi YEBO Proctology Hospital of Traditional
Chinese Medicine, Wuxi, PR China

Correspondence
Huanhuan Zhu, Department of Anorectal
Surgery, Wuxi Traditional Chinese Medicine
Hospital, No. 8 Zhongnan West Road, Binhu
District, Wuxi City, Jiangsu Province, 214071,
PR China
Email: zhuhuanhuan_wxzyy@163.com

Abstract

Tanshinol (TAN) is a widely used Chinese medicine ingredient with anti-inflammatory activity. The therapeutic effect of TAN in ulcerative colitis (UC) deserves further investigation. DSS induced UC model for mice, and TAN of different concentrations was used for in vivo therapy. Colons length was measured; expression of VLDLR in colonic mucosal tissue was evaluated by qRT-PCR, Western blot and histochemical staining. Besides, normal colorectal mucosal cell line (FHC) was treated with LPS to imitate the inflammatory process of UC in vitro. Different concentrations of TAN treated UC cell model. ELISA and qRT-PCR were applied to examine the concentrations of inflammatory cytokines (TNF-α, IL-6, IL-8, or IL-1β). Flow cytometry and MTT was used to identify the apoptosis and viability of FHC cells, respectively. Afterwards, Western blot was performed to detect the expressions of Bax, Bcl-2, Cleaved caspase-3, and Cleaved caspase-9 in FHC cells. VLDLR was low-expressed in UC tissues as compared to the normal tissue. TAN could alleviate DSS-induced colons length shortening, colonic tissue structure destruction, inflammatory response, and VLDLR expression decrease in vivo. Further study found that TAN could alleviate LPS-induced inflammatory response, apoptosis, and viability decrease of FHC cells, and siVLDLR could partially offset the effect of TAN. TAN alleviates LPS-induced viability decrease, apoptosis, and inflammatory response in FHC cells by promoting VLDLR expression.

KEYWORDS
apoptosis, inflammation response, tanshinol, ulcerative colitis, viability

1 | INTRODUCTION

Ulcerative colitis (UC) is a type of inflammatory bowel disease (Seyedian et al., 2019). It is a chronic idiopathic disease caused by abnormal immune response of host gastrointestinal flora (Franzosa et al., 2019), characterized by uncontrolled inflammation of the colon

and rectum (Nunes et al., 2019). At present, the incidence of UC shows a rapid rise, especially in developing countries (Pillai et al., 2019). The treatment for UC is mainly to reduce the inflammatory reaction with drugs. 5-amino Salicylic acid is usually selected as the therapeutic drug in UC treatment for its anti-inflammatory effects, however, adverse reactions would generated under this treatment in

a long term (Piodi et al., 2004). As a natural medicine component, traditional Chinese medicine (TCM) ensures the safety of drugs, and shows its unique advantages. Consequently, the search for novel effective TCM drugs to treat UC is helpful to improve the clinical overcome of this disease.

Danshen (*Salvia miltiorrhiza*) is a plant in the Labiatae family (Moon & Cha, 2020). It has the functions of activating blood circulation, removing blood stasis, cooling blood circulation, eliminating carbuncle, relieving pain, and nourishing blood and calming nerves (Zhang et al., 2020). Tanshinol (TAN) is one of the main active ingredients isolated from the root of *Salvia miltiorrhiza* and is now widely concerned for its antioxidant and anti-inflammatory properties in various diseases (Liu et al., 1999; Xing et al., 2014). TAN inhibits inflammatory factors in the vascular dementia model rat through the MST1-FOXO3 signaling pathway (Yang et al., 2016). However, whether TAN could alleviate UC is still unknown. According to study of Guo et al., dihydrotanshinone I improved experimental ulcerative colitis induced by DSS in mice (Guo et al., 2018). The main reason could be explained by the fact that dihydrotanshinone I and TAN are both the main active ingredients of salvia miltiorrhiza (Gao et al., 2018). It is reasonable to speculate that TAN could cure UC. Research indicated that TAN could significantly increase the expression of very low density lipoprotein receptor (VLDLR) (Chen et al., 2017). In fact, the gene expression profiles analyzed by GEO database (GSE87473) about normal and UC patients also showed that VLDLR expression was significantly reduced in UC patients. Therefore, we hypothesized that TAN might alleviate UC by promoting VLDLR.

In this study, the expression of VLDLR in UC tissues and normal tissues was firstly tested. Next, in order to explore the effect of TAN in UC, we induced UC in mice with Dextran sulfate sodium salt (DSS) and induced UC related inflammatory processes in normal colorectal mucosal cell line (FHC) with lipopolysaccharide (LPS). Loss of VLDLR expression was used to verify whether TAN treatment of UC via regulating VLDLR expression. This study aims to provide a potential therapeutic agent for the treatment of UC.

2 | MATERIALS AND METHODS

2.1 | Ethics statement

The tissues used in this study were derived from 35 UC patients and 12 normal volunteers confirmed in Wuxi Traditional Chinese Medicine Hospital from Sep. 2018 to Jun. 2019. All patients and volunteers signed informed consent and agreed that their organizations would be used in the study. Part of the animal experiments in this study strictly follow guidelines of the China Council on Animal Care and Use, and try to reduce the discomfort and pain of experimental animals during the experiment. This study has been approved by the Ethics Committee of Wuxi Traditional Chinese Medicine Hospital (WX201812372) (WX201909371).

2.2 | Mice modeling and treatment

Forty C57BL/6J male mice (age, 6 week; weight, 16–19 g) were purchased from the Beijing Vital River Laboratory Animal Technology Co., Ltd. (Beijing, China). Mice were raised under standard environment conditions of 25°C, 55–65% humidity and 12 h light/dark cycle, and had free access to sterilized water and standard food. Mice were acclimatized for 1 week prior to modeling. All mice were randomly divided into four groups, namely control group (10 mice, normal mice), model group (10 mice, model mice), model + 15 group (10 mice, model mice treated with 15 mg/kg TAN), and model + 30 group (10 mice, model mice treated with 30 mg/kg TAN). Mice in the control group were normal diet, and mice in the model group drank water containing 5% DSS for 7 consecutive days (Guo et al., 2018; Yan et al., 2018). During this duration, mice in the control and model groups were given 10 ml of normal saline once every 2 days for 14 consecutive days, and model + TAN group was given 15 mg/kg or 30 mg/kg TAN (44,884, National Institutes for Food and Drug Control, Beijing, China; dissolved in 10 ml of normal saline) once every 2 days for 14 consecutive days (Chen et al., 2017; Guo et al., 2018). On day 14, the mice were sacrificed by injecting 60 mg/kg sodium pentobarbital and the colon tissue was taken to measure the length.

2.3 | Histochemical staining

The paraffin-embedded UC tissues or normal tissues were cut into 2 μm sections. First, the sections were placed in xylene twice (10 min for each time) and then dehydrated in gradient alcohol (70%, 80%, 90%, and 100%) (5 min for each time). For immunohistochemistry (IHC), the sections were boiled twice (8 min for each time) in 10 mM sodium citrate buffer solution (P0081, Beyotime, Shanghai, China) to repair the antigen, and then incubated with 3% hydrogen peroxide for 10 min. Then, 10% goat serum (C0265, Beyotime, Shanghai, China) was used to seal the sections for 1 h at room temperature. Afterwards, the sections were dripped with primary antibody (VLDLR: ab203271, 1:300, Abcam, Cambridge, MA) and incubated in a wet box at 4°C overnight. The second day, the primary antibody was removed, and the second antibody (Goat Anti-Rabbit IgG H&L (HRP): ab6721, 1:1000, Abcam) was added to the mixture for 1 h at room temperature. The sections were then stained with DAB kit (P0203, Beyotime, China) and restained with hematoxylin (C0107, Beyotime, Shanghai, China). For H&E staining, the sections were dyed in the hematoxylin dye solution for 10 min and then differentiated with the differentiation liquid for 30s. Flush with tap water for 15 min and then use eosin for 30 s. Afterwards, the above sections were dehydrated with conventional gradient alcohol (100%, 90%, 80%, and 70%) (5 min for each time) and permeated with xylene (10 min for each time). Finally, the film was sealed with neutral glue (G8509, Solarbio, Beijing, China), observed and photographed under an inverted microscope (×100, ×200; POMEAS, Guang dong, China).

2.4 | Cell culture and treatment

Normal colorectal mucosal cell line (FHC) were obtained from American Type Culture Collection (ATCC, Rockville, MD) and cultured in F12-DMEM (12400-024, Gibco, Grand Island, NY) supplemented with 10% fetal bovine serum (FBS, 10099-141, Gibco) and 1% penicillin/streptomycin (15070063, Gibco, Grand Island, NY) in an incubator (37°C, 5% CO_2).

LPS (L4391, Sigma-Aldrich, St. Louis, MO, USA) was dissolved with ultrapure water and the final concentration of LPS is 5 mg/ml. The environment of UC was simulated by adding 8 ng/ml LPS into FHC cells.

TAN was dissolved in PBS and a 10 mM solution was prepared. Then, TAN (25, 50, 100 μmol/L) was added to LPS-treated FHC cells for 30 min as treatment group.

2.5 | Cell transfection

siVLDLR (5′-AGATCGTAGGATAGTACTAAA-3′) and siNC was designed and conducted by Genephama (Shanghai, China). Then, Lipofectamine 2000 (Lipo2000) (11668-027, Invitrogen, Carlsbad, CA) was used as a transfection reagent to transfect siVLDLR or siNC into FCH cells. Briefly, 50 pmol of siVLDLR or siNC and 5 μl of Lipo2000 were added to 125 μl of Opti-MEM (31985088, Gibico, Grand Island, NY), respectively. After 5 min, two mixtures were mixed and then add to the corresponding cells after 20 min. Fresh media was added 6 h post-transfection. Cells were continued to culture in an incubator with 5% CO_2 in 37°C.

2.6 | MTT assay

Transfected or untransfected FHC cells were planted in 96-well plates with 1000 cells/well. After 24 h, the cells were treated with or without LPS and TAN, and then the cell viability of each treatment group was detected with MTT kit (C0009, Beyotime, China) after 24 h. Briefly, 20 μl MTT (5 mg/ml) was added to each well for 2 h at 37°C. Removed the culture medium, the hole of the culture plate was add with 200 μl DMSO (ST038, Beyotime, Shanghai, China). OD value at 570 nm was detected by a microplate reader (Molecular Devices, Sunnyvale, CA) after shaking with shaking table for 5 min.

2.7 | Flow cytometry

Transfected or untransfected FHC cells were planted in 6-well plates with 2×10^5 cells/well. After 24 h, the cells were treated with or without LPS and TAN, and then Annexin V-FITC kit (Bectin, Dickinson and Company, Franklin Lakes, NJ) was used to detect apoptosis. Briefly, the cells were digested with trypsin (25200056, Gibico) and transferred to the flow tube. Afterwards, the cells washed with PBS for two times, and resuspended with 100 μl of binding buffer. Subsequently, 5 μl of Annexin V-FITC and PI were added to the tube, and

incubated in the dark for 15 min. Cell apoptosis was detected by flow cytometry (Beckman Coulter, CA) within 30 min.

2.8 | Enzyme-linked immunosorbent assays (ELISA)

The above colon tissues were added with tissue extraction reagent. After homogenizing, the supernatant was removed by centrifugation (10,000g, 5 min, 4°C). ELISA kits (TNF-α, E-EL-M0044c; IL-1β: E-EL-M0037c; IL-6: E-EL-M0044c; Elabscience, Wuhan, China, https://www.elabscience.cn/) were used to detect the levels of TNF-α, IL-1β, and IL-6 in the supernatant (ng/g). Transfected or untransfected FHC cells were planted in 6-well plates with 2×10^5 cells/well. After 24 h, the concentrations of IL-1β, IL-6, and IL-8 in the FHC supernatant (pg/ml) were detected by ELISA kits (IL-1β: E-EL-H0149c; IL-6: E-EL-H0102c; IL-8: E-EL-H6008) according to the instructions. The ELISA kit was taken out of the refrigerator at 4°C and balanced at room temperature for 30 min. Standard group (six concentration), blank group, and sample group to be tested, and sample added were as follows: 100 μl standard solution was added to blank hole as standard solution; 100 μl of distilled water were then added to the blank control hole. The remaining holes were filled with 100 μl of sample and used for further testing. Fifty microliters hydrogen peroxide cresol solution was added to each hole of the standard group and the sample group to be tested. Then the label board was sealed with sealing paper, incubated at 37°C for 1 h. After the end of incubation, each hole was filled with diluted dishwashing liquid solution and stood for 30 s. Clean the label board thoroughly for five times and pat the paper dry. Chromo-developing solution A (50 μl) and chromo-developing solution B (50 μl) were add to each hole, respectively. Then, 50 μl termination solution was added to the hole at room temperature for 15 min. OD value of each hole at 450 nm was measured by a microplate reader.

2.9 | Quantitative reverse transcription polymerase chain reaction (qRT-PCR)

Total RNA was extracted from FHC cells or tissues with TRIZOL reagent (R0016, Beyotime, Shanghai, China). Then, the total RNA was reverse transcribed by a High Capacity cDNA Reverse Transcription Kit (4374966, Invitrogen, USA). In order to detect the mRNA expression levels of VLDLR, IL-6, IL-8, and IL-1β, the SYBR® Fast qPCR Mix kit (RR036A, Takara, Dalian, China) was used for qPCR. GAPDH was used as an internal reference. The reaction system of qPCR was as follows: 1 μg of cDNA, 10 μl of SYBR Premix Ex TaqII™ (2×), 0.2 mol/L of each primer (Primers were designed and conducted by Sangon Biotech, as list in Table 1.) and then added ultra-pure water to 20 μl. The reaction conditions of qPCR were as follows: 95°C, 3 min; The 40 cycles included: 95°C, 30 s and 60°C, 15 s. The data of qPCR were calculated by $2^{-\Delta\Delta t}$ method (Livak & Schmittgen, 2001).

TABLE 1 Specific primer sequences for quantitative reverse transcription polymerase chain reaction

Gene	Primer sequence	Species
VLDLR	5′-CTGTGTAAAGAAGACGTGTGCT-3′ 5′-TGATTTCATGTATGCGGCATGT-3′	Human
VLDLR	5′-GAGTCTGACTTCGTGTGCAAA-3′ 5′-GAACCGTCTTCGCAATCAGGA-3′	Mice
IL-6	5′-ACTCACCTCTTCAGAACGAATTG-3′ 5′-CCATCTTTGGAAGGTTCAGGTT-3′	Human
IL-8	5′-TTTTGCCAAGGAGTGCTAAAGA-3′ 5′-AACCCTCTGCACCCAGTTTTC-3′	Human
IL-1β	5′-ATGATGGCTTATTACAGTGGCAA-3′ 5′-GTCGGAGATTCGTAGCTGGA-5′	Human
GAPDH	5′-ACAACTTTGGTATCGTGGAAGG-3′ 5′-GCCATCACGCCACAGTTTC-3′	Human

2.10 | Western blot

Total proteins from FHC cells or tissues were extracted by the RIPA reagent (P0013B, Beyotime, China) (containing 1% phenylmethanesulfonyl fluoride (PMSF, P1030, Beyotime, China) and 2% phosphatase inhibitor (P1081, Beyotime, China)). The protein content of the sample was determined by BCA kit (P0012, Beyotime, China). Equal quantities of 30 μg of total protein and marker (PR1910, Solarbio, China) were separated by SDS-PAGE (P0012A, Beyotime, China) electrophoresis. The protein samples were then transferred to the PVDF membrane (ISEQ00010/IPVH00010, MILLIPORE, USA), and 5% skim milk (232100, B&D, USA) was used to block the membrane. After closure, the membrane was washed by TBST (TBS plus 0.1% Tween) for 5 min and incubated in the primary antibodies (Bcl-2 associated X (Bax): ab32503, 1:5000, Abcam; B-cell lymphoma-2 (Bcl-2): ab59348, 1:1000, Abcam; Cleaved caspase 9: #20750, 1:1000, CST; Cleaved caspase 3: ab49822, 1:500, Abcam; VLDLR: ab203271, 1:1000, Abcam; GAPDH: ab8245, 1:10,000, Abcam) at 4°C overnight. On the second day, the primary antibodies were recovered and washed with TBST for four times (5 min for each time), and then transferred to the secondary antibody (Goat Anti-Rabbit IgG H&L (HRP): ab6721, 1:1000, Abcam) for 1 h of incubation at room temperature. Afterwards, the membrane was washed again with TBST for four times (5 min for each time). The enhanced chemiluminescence solution (ECL, WBKLS0500, MILLIPORE, USA) was used to drip onto the protein strips and visualize the strips using a detection system (Bio-RAD, CA). The gray value of the strip was analyzed with image J (1.8.0, National Institutes of Health, Germany).

2.11 | Statistical analysis

Statistical analyses were performed by GraphPad Prism software 8.0 (GraphPad Software, San Diego, CA), and measurement data were expressed as mean ± standard deviation (SD). Independent samples t-test was used in the comparisons between two groups. One-way ANOVA with post-hoc Tukey multiple comparisons was used to compare multiple groups. $P < .05$ was considered as statistically significant.

3 | RESULT

3.1 | VLDLR was low-expressed in UC tissues

First, immunohistochemistry, qRT-PCR, and Western blot were performed to measure the expression of VLDLR in UC and normal tissues. According to Figure 1a, compared with the large area of VLDLR antibody labeled gray in normal tissue, the UC tissue presented less gray. Then, qRT-PCR detected that the mRNA expression of VLDLR in human UC tissues was significantly lower than that in normal tissues (Figure 1b, $P < .001$), and Figure 1c,d presented that the protein expression of VLDLR in human UC tissues was also lower than normal tissues ($P < .001$).

3.2 | TAN alleviated LPS-induced cell viability decrease and inflammatory response

Figure 2a showed the chemical structure of TAN. MTT assay was performed to determine the dosage of TAN that exerted nontoxicity on cells, and results showed that when the TAN concentration reached 200 μmol/L, the viability of FHC cells was decreased (Figure 2b, $P < .05$). Thus, we chose the concentration of 25, 50, and 100 μmol/L of TAN as the experimental concentration. LPS could induce inflammation, and we chose 8 μg/ml of LPS to treat FCH cells according to a previous study (Qiao et al., 2019). As expected, LPS not only reduced the viability of FHC cells, but also promoted the expressions of IL-6, IL-8, and IL-1β (Figure 2c–i, $P < .05$, $P < .01$, $P < .001$). Afterwards, we performed TAN therapy on LPS treated FHC cells, and found that TAN inhibited LPS-induced cell viability decrease and inflammatory factors (IL-6, IL-8, and IL-1β) expressions (Figure 2c–i). The effect of TAN was concentration dependent.

3.3 | TAN alleviated LPS-induced FHC cell apoptosis and VLDLR expression decrease

LPS-treated FHC cells enhanced apoptosis as compared to the control group (Figure 3a, $P < .001$). Further detection of apoptotic proteins (Bax, Bcl-2, Cleaved caspase-3, Cleaved caspase-9) expressions also showed that LPS enhanced apoptosis of FHC cells. As evidenced by the Figure 3b–f, LPS enhanced the expressions of Bax, cleaved caspase-3, and cleaved caspase-9, while decreased the Bcl-2 expression (Figure 3b–f). Fortunately, TAN alleviated LPS-induced apoptosis of FHC cells in a concentration-dependent manner (Figure 3b–f, $P < .05$, $P < .001$). Afterwards, we examined the effect of TAN on the expression of VLDLR. Data in Figure 3g–i suggested that LPS decreased the expression of VLDLR in FHC cells in comparation to the control group. However, TAN could partially reverse LPS-inhibited the VLDLR expression (Figure 3g–i, $P < .001$).
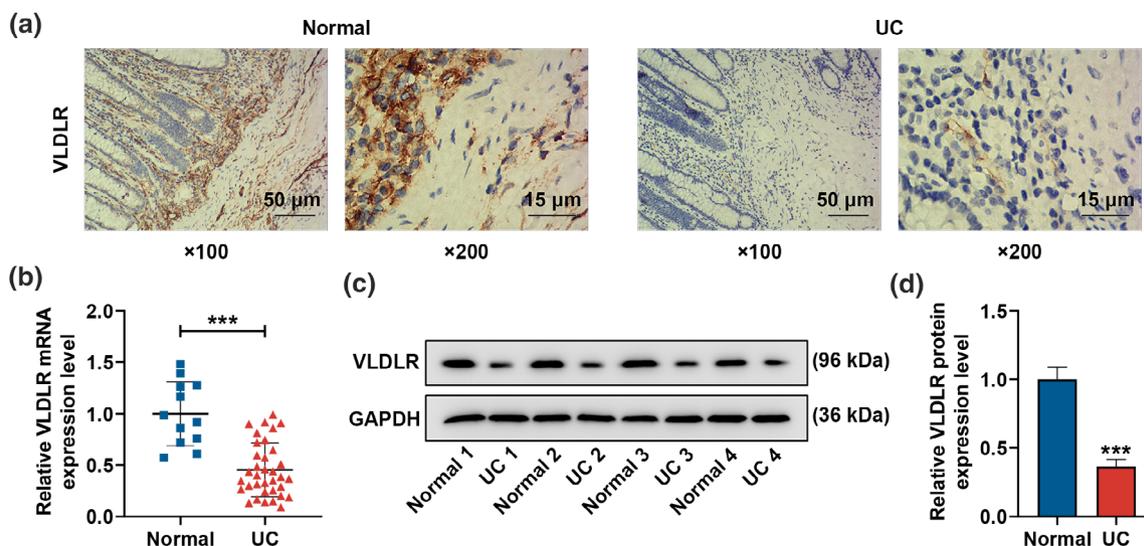
FIGURE 1 VLDLR was low-expressed in UC tissues. (a) Immunohistochemistry was used to detect VLDLR expression in colonic mucosal tissues of UC patients and normal controls. Scales: 50 and 15 μm; magnifications: ×100 and ×200. (b) The expression of VLDLR in colonic mucosal tissues of UC patients and normal controls was detected by qRT-PCR. GAPDH severs as an internal reference. (c) The expression of VLDLR in colonic mucosal tissues of UC patients and normal controls was detected by Western blot. (d) Gray value analysis of Western blot results. GAPDH severs as an internal reference. * Vs. Normal; ***$P < .001$. UC, ulcerative colitis; qRT-PCR, quantitative reverse transcription polymerase chain reaction; VLDLR, low density lipoprotein receptor
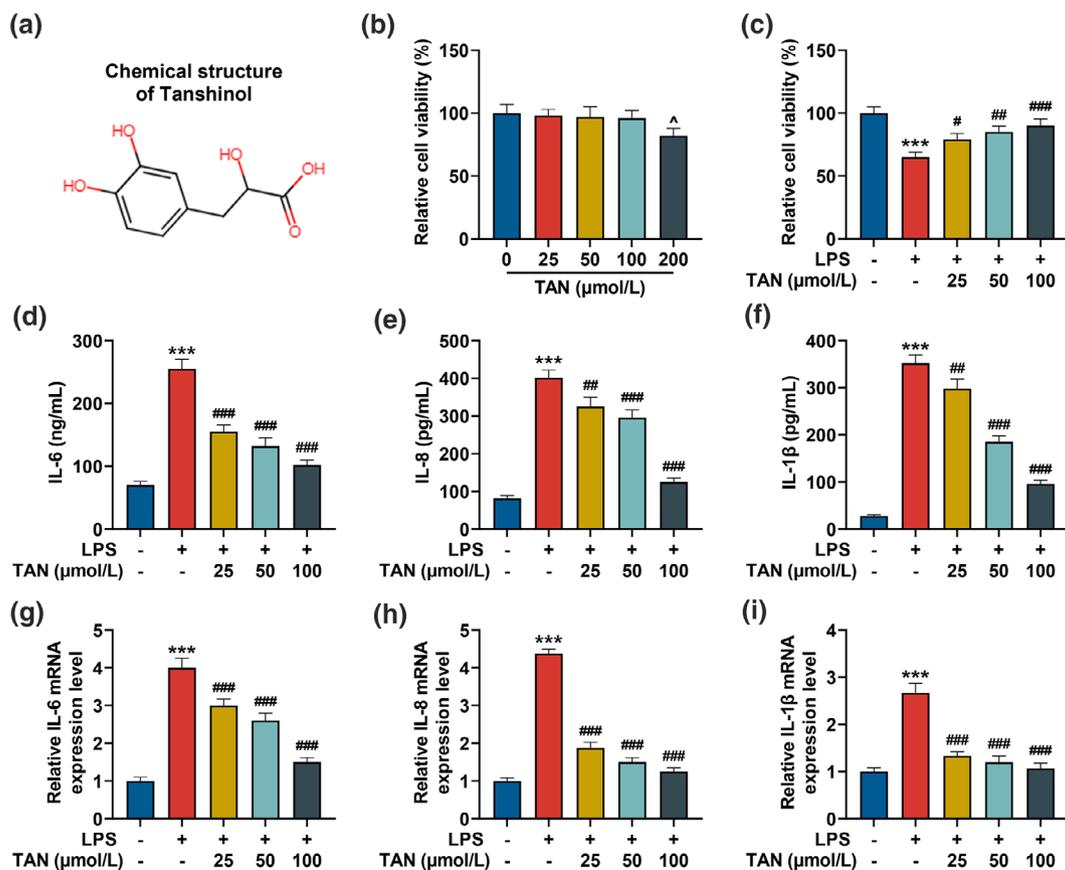

FIGURE 2 TAN alleviated LPS-induced cell viability decrease and inflammatory response. (a) The chemical structure of TAN. (b) MTT was used to detect the cell viability of FHC cells treated with different concentrations of TAN. (c) MTT was used to detect the cell viability of FHC cells treated with or without LPS and TAN. (d–f) ELISA was used to measure the content of IL-6, IL-8, IL-1β in FHC cells treated with or without LPS and TAN. (g–i) qRT-PCR was used to identify the expressions of IL-6, IL-8, IL-1β in FHC cells treated with or without LPS and TAN. No treatment group was set as control groups. GAPDH severs as an internal reference. * Vs. control, # vs. LPS; ***$P < .001$, #$P < .05$, ##$P < .01$, ###$P < .001$. TAN, tanshinol; LPS, lipopolysaccharide; MTT, 3-[4,5-Dimethylthiazol-2-yl]-2,5-diphenyltetrazolium bromide; qRT-PCR, quantitative reverse transcription polymerase chain reaction; IL, interleukin; FHC, normal colorectal mucosal cell line
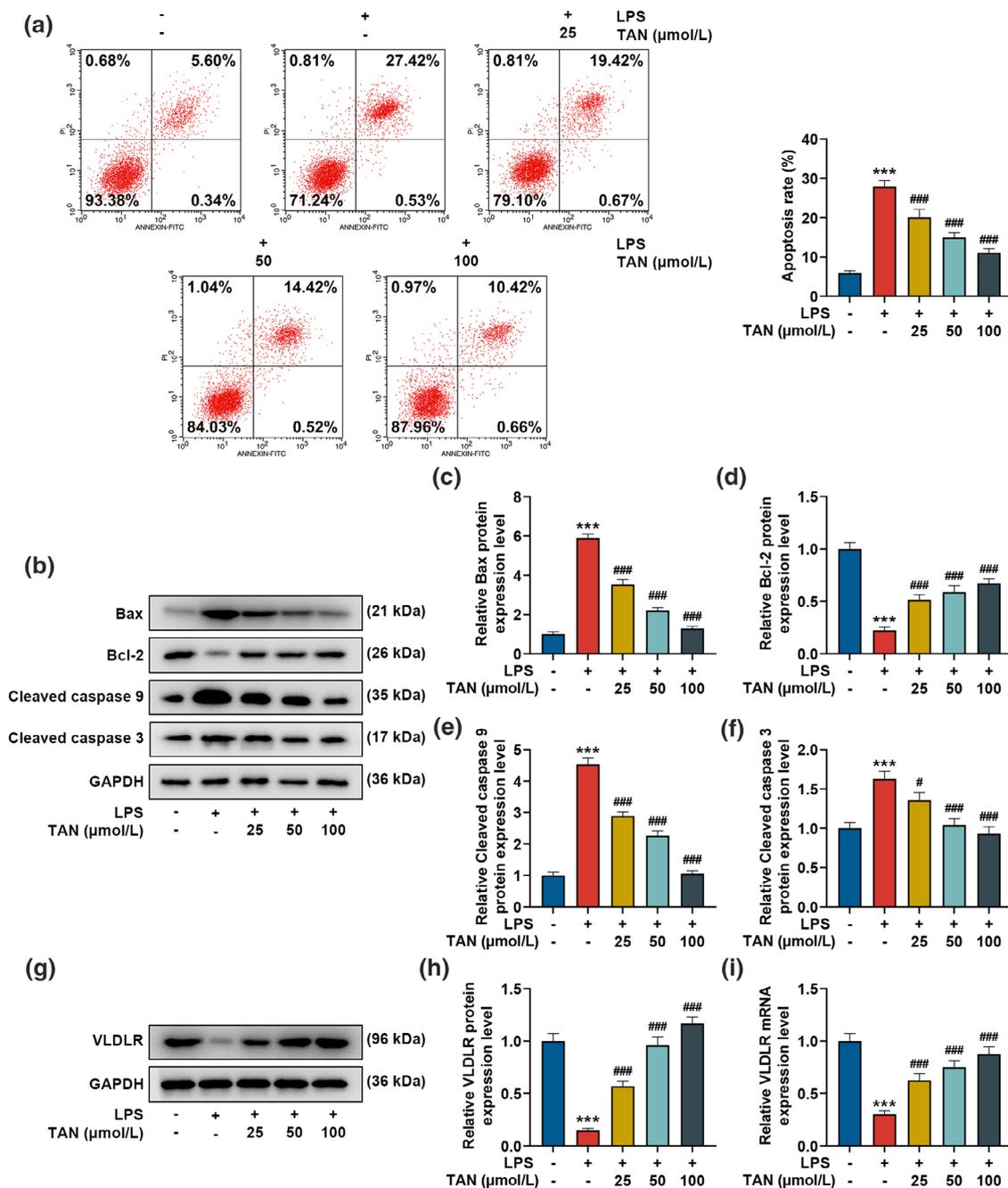
FIGURE 3 TAN alleviated LPS-induced FHC cells apoptosis. (a) Flow cytometry was used to detect the cell apoptosis of FHC cells treated with or without LPS and TAN. (b, g) The expressions of Bax, Bcl-2, cleaved caspase-3, cleaved caspased-9 and VLDLR in of FHC cells treated with or without LPS and TAN was detected by Western blot. (c–f, h) Gray value analysis of Western blot results. (i) qRT-PCR was used to detect the expressions of VLDLR in FHC cells treated with or without LPS and TAN. GAPDH severs as an internal reference.* Vs. control, # vs. LPS; ***$P < .001$, ###$P < 0.001$. TAN, tanshinol; LPS, lipopolysaccharide; Bax, Bcl-2 associated X; Bcl-2, B-cell lymphoma-2; FHC, normal colorectal mucosal cell line

3.4 | Silencing VLDLR partially reversed the effect of TAN on the viability and inflammatory response of LPS-induced FHC cell

From our experimental results, TAN could enhance the expression of VLDLR in UC model in vitro. Therefore, we wanted to verify whether TAN could achieve the mitigation effect on UC by promoting the expression of VLDLR. The transfection efficiency of siVLDLR was

measured by qRT-PCR and Western blot. As shown in Figure 4a–c, siVLDLR could significantly reduce the expression of VLDLR as compared to the control group, both at the protein and mRNA levels ($P < .01$, $P < .001$). First, we found TAN could alleviate LPS-induced cell viability decrease, while siVLDLR partially offset the effect of TAN on cell viability (Figure 4d, $P < .05$, $P < .01$, $P < .001$). Then, we tested the effects of TAN and VLDLR on the expressions of inflammatory cytokines (IL-6, IL-8, and IL-1β). The results of
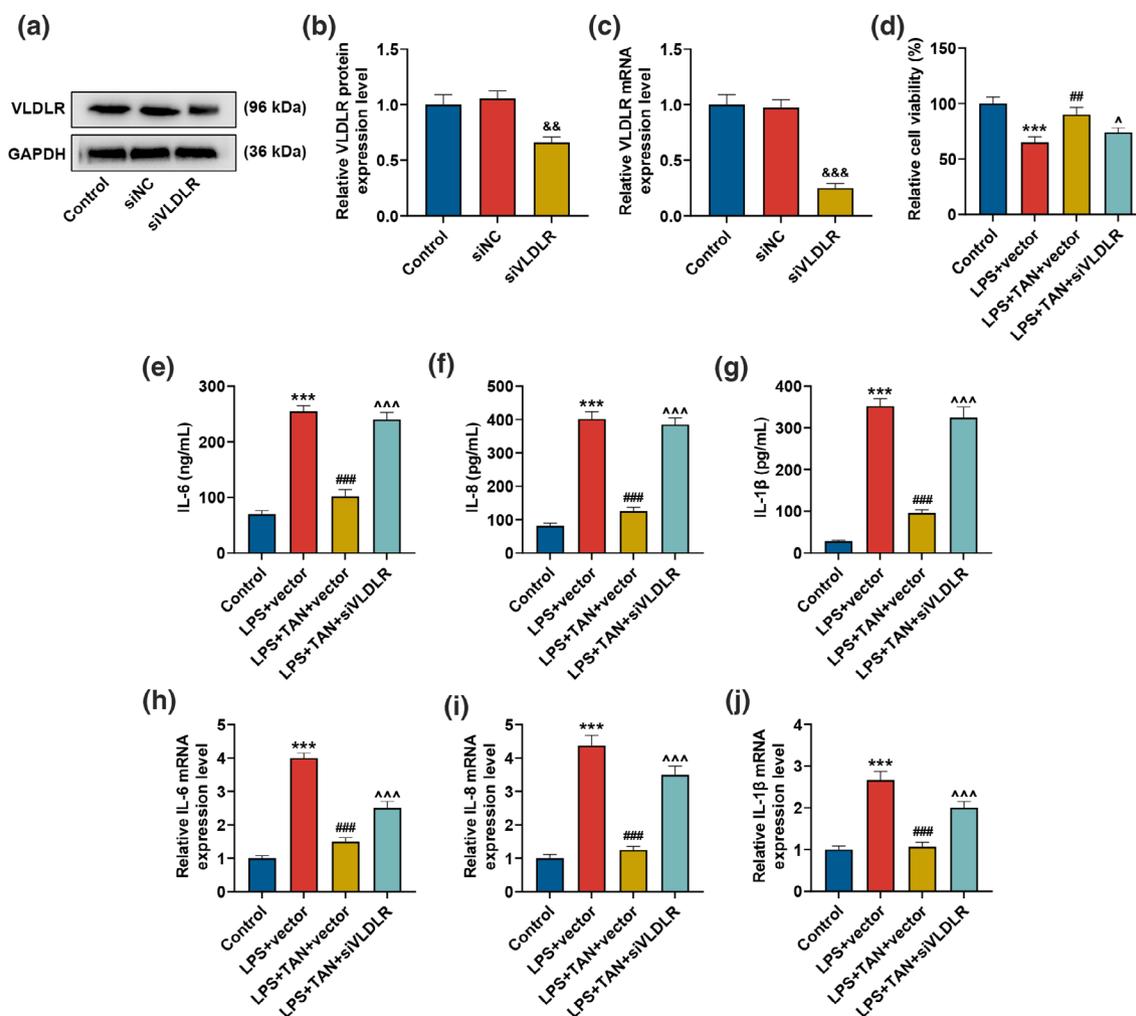
FIGURE 4 TAN alleviated LPS-induced cell viability decrease and inflammatory response by promoting VLDLR expression. (a) Western blot was used to detect the transfection efficiency of siVLDLR. (b) Gray value analysis of Western blot results. (c) qRT-PCR was used to detect the transfection efficiency of siVLDLR. (d) MTT was used to detect the cell viability of FHC cells treated with or without siVLDLR, LPS and TAN. (e–g) ELISA was used to measure the content of IL-6, IL-8, IL-1β in FHC cells treated with or without siVLDLR, LPS and TAN. (h–j) qRT-PCR was used to identify the expressions of IL-6, IL-8, IL-1β in FHC cells treated with or without siVLDLR, LPS and TAN. GAPDH severs as an internal reference. $^{\&}$ Vs. siNC, * vs. control, $^{\#}$ vs. LPS + vector, $^{\wedge}$vs. LPS + TAN + vector; $^{\&\&}P < .01$, $^{***}P < .001$, $^{\#\#\#}P < .001$, $^{\wedge\wedge\wedge}P < .001$. qRT-PCR, quantitative reverse transcription polymerase chain reaction; MTT, 3-(4,5-Dimethylthiazol-2-yl)-2,5-diphenyltetrazolium bromide; TAN, tanshinol; IL, interleukin; VLDLR, low density lipoprotein receptor; ELISA, enzyme-linked immunosorbent assays; FHC, normal colorectal mucosal cell line

ELISA and qRT-PCR both showed that TAN could reduce LPS-induced the expression of IL-6, IL-8, and IL-1β, while siVLDLR could partially reverse the regulatory effect of TAN (Figure 4e–j, $P < .001$).

3.5 | Silencing VLDLR partially reversed the effect of TAN on the apoptosis of LPS-induced FHC cell

The effects of TAN and siVLDLR on apoptosis of LPS-treated FHC cells were detected by flow cytometry. LPS-induced FHC cells apoptosis could be significantly alleviated by TAN, while siVLDLR could partially alleviate the effect of TAN (Figure 5a, $P < .001$). To further confirm this result, we also measured expressions of apoptotic proteins (Bax, Bcl-2, cleaved Caspase-3, and cleaved Caspase-9). Results

showed that TAN could mitigate LPS-induced increases of Bax, cleaved Caspase-3, cleaved Caspase-9, and decreases of Bcl-2 expressions (Figure 5b–f, $P < .001$). Interestingly, siVLDLR partially reversed the effect of TAN on the expressions of apoptotic proteins (Figure 5b–f, $P < .001$). This suggests that TAN alleviated LPS-induced apoptosis of FHC cells by promoting the expression of VLDLR.

3.6 | TAN alleviated inflammatory response of the DSS-induced UC model mice

The survival rate of mice was recorded, DSS exposed result in a survival rate of 40%, whereas TAN improved the survival rate of mice (Figure 6a). From our measurements of colons length in mice, the UC model mice had shorter colonic length than the control group, and
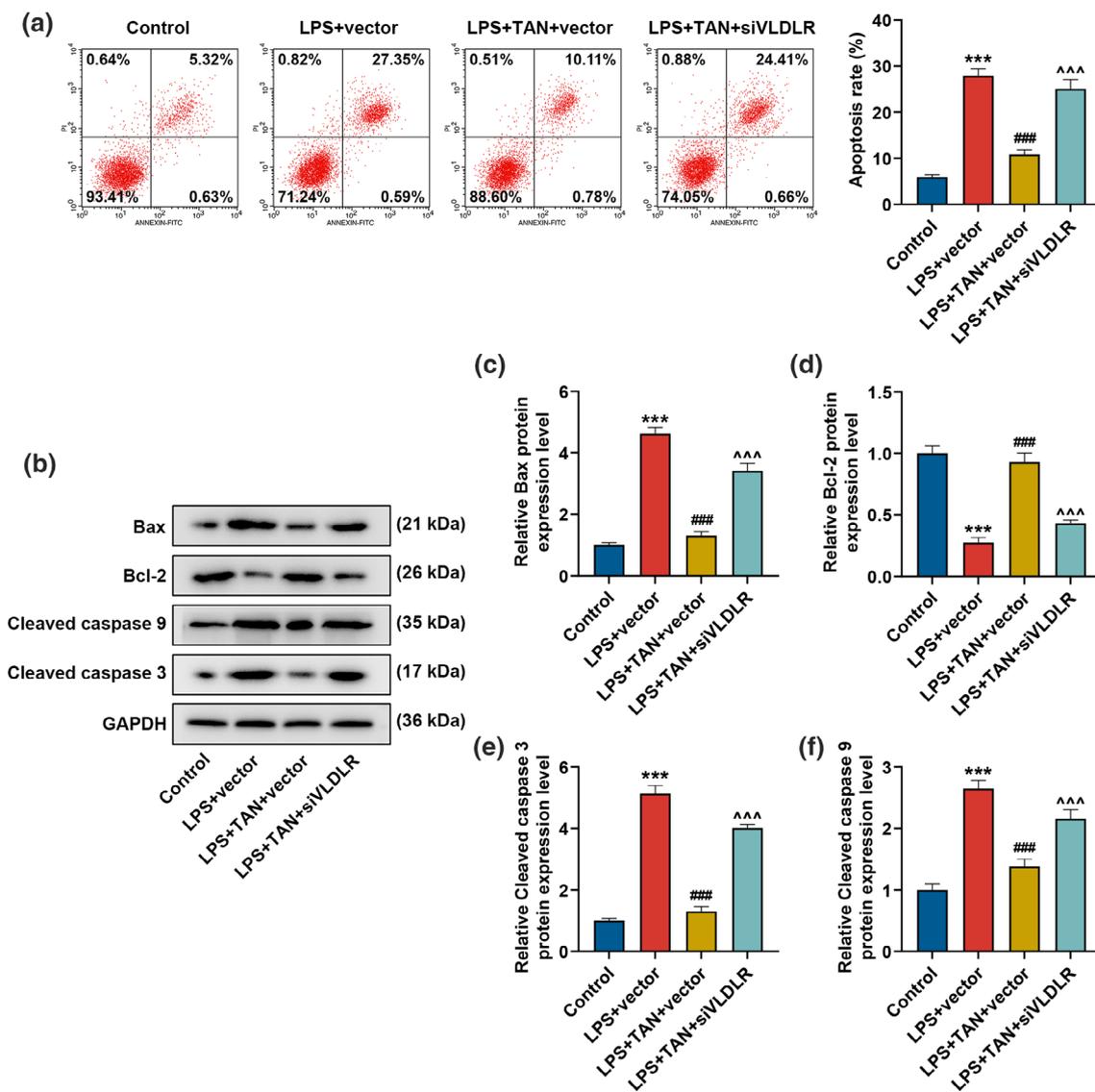
FIGURE 5 TAN alleviated LPS-induced FHC cell apoptosis by promoting VLDLR expression. (a) Flow cytometry was used to detect the cell apoptosis of FHC cells treated with or without siVLDLR, LPS and TAN. (b) The expressions of Bax, Bcl-2, cleaved caspase-3 and cleaved caspased-9 in FHC cells treated with or without siVLDLR, LPS and TAN was detected by Western blot. (c–f) Gray value analysis of Western blot results. GAPDH severs as an internal reference. * Vs. control; # vs. LPS + vector; ^ vs. LPS + TAN + vector; ***$P < .001$, ###$P < .001$, ^^^$P < .001$. TAN, tanshinol; LPS, lipopolysaccharide; Bax, Bcl-2 associated X; Bcl-2, B-cell lymphoma-2; VLDLR, low density lipoprotein receptor; FHC, normal colorectal mucosal cell line

TAN was able to alleviate colons shortening in model mice (Figure 6b, $P < .05$, $P < .01$, $P < .001$). Afterwards, colonic tissue was stained by H&E. Compared with normal colonic tissue in the control group, the colonic tissue of UC model mice was damaged, with edema and inflammatory cell infiltration in the muscle layer (Figure 6c). However, TAN alleviated the damage of colon tissue in UC model mice in a concentration-dependent manner (Figure 6c). In addition, TAN reduced the levels of TNF-α, IL-6, and IL-1β in the colon tissue of UC model mice (Figure 6d–f, $P < .001$). Moreover, the expression of VLDLR was decreased in model group, but TAN increased the VLDLR expression (Figure 6g–h, $P < .001$).

4 | DISCUSSION

UC is a chronic inflammatory disease of the intestinal tract, which often involves mucosa and submucosa (Tatiya-Aphiradee et al., 2018). To date, there has been no effective medical treatment for UC, and the etiology is poorly understood. Thus, it is of great significance to find new drugs and their target molecules for the treatment of UC. Fortunately, growing evidences showed that TCM could inhibit the development of UC by acting on key target molecules in the process of UC. Salvia miltiorrhiza is a traditional Chinese medicine, and its active ingredient TAN has been shown to treat a variety of diseases
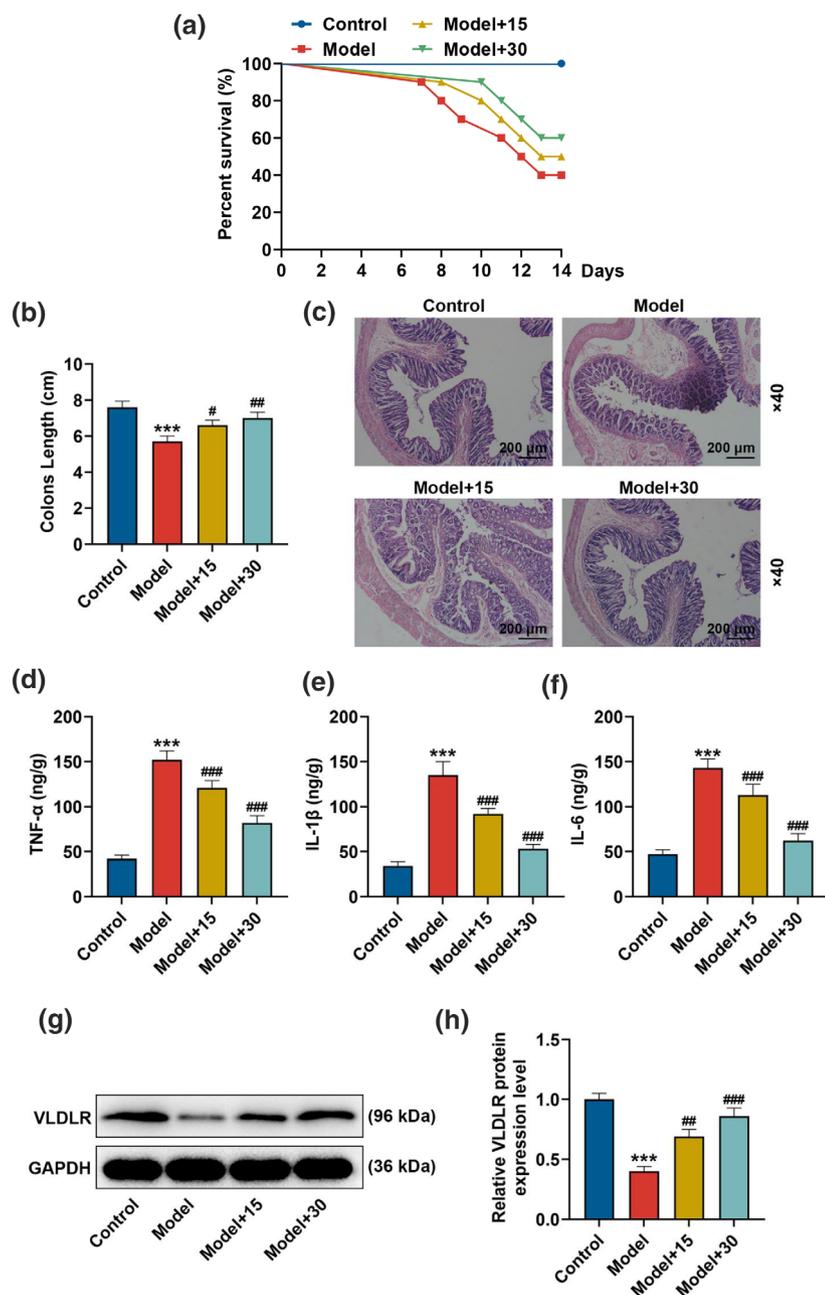
FIGURE 6 TAN alleviated DSS-induced UC and VLDLR expression decrease. (a) The survival rate of mice was recorded. (b) The colons length of mice was measured. (c) H&E staining of colonic tissue in mice. Scale: 200 μm; magnification: ×40. (d–f) The levels of TNF-α, IL-1β, and IL-6 in colon tissue were detected by ELISA. (g) The expression of VLDLR of mice colonic tissues was determined by Western blot. (h) Gray value analysis of Western blot results. GAPDH severs as an internal reference. [*] Vs. control, [#] vs. model. [#]$P < .05$; [##]$P < .01$, [***]$P < .001$, [###]$P < .001$. UC, ulcerative colitis; ELISA, enzyme-linked immunosorbent assays; VLDLR, low density lipoprotein receptor; H&E, hematoxylin–eosin staining

(Chen et al., 2017; Luo et al., 2018; Luo et al., 2019; Wang & Zhang, 2020; Zhu et al., 2019). However, there is currently no evidence that TAN has a therapeutic effect on UC. In our study, LPS-treated FHC cells showed a significant decrease in cell viability, and the expressions of inflammatory cytokines (IL-6, IL-8, and IL-1β) were significantly increased. Strikingly, TAN was able to alleviate LPS-induced cell viability decrease and inflammatory cytokine expression. TAN could also alleviate LPS-induced apoptosis of FHC cells. It is noteworthy that the increased expressions of IL-6, IL-8, and IL-1β are considered to be a marker of UC occurrence (Angelidou et al., 2018; Gupta et al., 2018; Walana et al., 2018). Besides, apoptosis-related proteins (Bax, Bcl-2, Cleaved caspase-3, and Cleaved caspase-9) were also implicated in UC. As reported by Seidelin et al., apoptosis-related proteins were well-expressed in UC (Seidelin & Nielsen, 2006). The

expressions of apoptosis-related proteins were also verified to determine the effect of TAN in UC and the results showed that TAN could decrease LPS-induced FHC cell apoptosis. Therefore, it can be seen that TAN could alleviate UC. However, the exact molecular mechanism of TAN in the treatment of UC remains to be elucidated. We then also demonstrated in vivo that TAN can alleviate DSS-induced colons length shortening, colonic lesions, and inflammatory responses.

In previous studies, VLDLR has been shown to be involved in regulating the occurrence of various diseases. Homozygous deletion mutation of VLDLR results in disequilibrium syndrome (DES) (a nonprogressive cerebellar ataxia with mental retardation) (Boycott et al., 2005). Besides, low expression of VLDLR could lead to arterial vascular lesions in atherosclerotic mice (Tan et al., 2018). In colon cancer (CRC), Kim et al. found that the expression of VLDLR in CRC

patients was lower than that in adjacent paired non-tumor tissues and VLDLR over-expression inhibited the proliferation and migration of CRC cells (Kim et al., 2017). Through immunohistochemical experiments, we found that the content of VLDLR in UC tissues was lower than that in normal tissues. The mRNA and protein expressions of VLDLR in tissues were further detected, and VLDLR was indeed down-regulated in UC. Perhaps VLDLR could be a therapeutic target for UC. To correlate and validate the results, we performed the detection of VLDLR in vitro. Since UC presents as a chronic recurrent inflammation confined to the colonic mucosa (Antonelli et al., 2018), human normal colonic mucosal cell line (FHC) was selected as the experimental subject. Then, FHC cells were treated with LPS to simulate the inflammatory damage caused by UC. Stimulation with LPS alone is sufficient to induce the inflammatory phenotype (Vijayan et al., 2019). The qRT-PCR and Western blot showed that LPS could inhibit the expression of VLDLR in FHC cells without incident. These results indicate that VLDLR is low expressed in UC.

Furthermore, Li et al. proved that TAN could significantly increase the expression of VLDLR (Chen et al., 2017). Similarly, our results also showed that TAN could reverse LPS-inhibited VLDLR expression. Therefore, we hypothesized that TAN alleviated UC by promoting the expression of VLDLR. In order to verify the above speculation, siVLDLR was selected to inhibit the expression of VLDLR. We found that siVLDLR could partially offset the effect of TAN in cell viability, inflammatory response and apoptosis of UC.

To sum up, our study found that the expression level of VLDLR was significantly reduced in LPS-induced FHC cells, while TAN could promote the expression of VLDLR. Down-regulated VLDLR reduced the TAN-induced promotion of cell activity and inhibition to cell apoptosis. It can be seen that TAN protects FHC cells from LPS-induced cell viability decrease, and inflammatory response and apoptosis are achieved by promoting the expression of VLDLR. TAN may be a potential therapeutic drug for UC.

CONFLICT OF INTEREST

The authors declare that they have no competing interests.

AUTHOR CONTRIBUTIONS

Substantial contributions to conception and design: Huanhuan Zhu. Data acquisition, data analysis, and interpretation: Shaopeng Tong, Yan Cui, Xiaodong Wang, Minying Wang. Drafting the article or critically revising it for important intellectual content: Huanhuan Zhu. Final approval of the version to be published: Huanhuan Zhu, Shaopeng Tong, Yan Cui, Xiaodong Wang, Minying Wang. Agreement to be accountable for all aspects of the work in ensuring that questions related to the accuracy or integrity of the work are appropriately investigated and resolved: Huanhuan Zhu, Shaopeng Tong, Yan Cui, Xiaodong Wang, Minying Wang.

DATA AVAILABILITY STATEMENT

The analysed data sets generated during the study are available from the corresponding author on reasonable request.

ORCID

Huanhuan Zhu https://orcid.org/0000-0003-3346-9123

REFERENCES

Angelidou, I., Chrysanthopoulou, A., Mitsios, A., Arelaki, S., Arampatzioglou, A., Kambas, K., Ritis, D., Tsironidou, V., Moschos, I., Dalla, V., Stakos, D., Kouklakis, G., Mitroulis, I., Ritis, K., & Skendros, P. (2018). REDD1/autophagy pathway is associated with neutrophil-driven IL-1β inflammatory response in active ulcerative colitis. *Journal of Immunology*, *200*(12), 3950–3961. https://doi.org/10.4049/jimmunol.1701643

Antonelli, E., Villanacci, V., & Bassotti, G. (2018). Novel oral-targeted therapies for mucosal healing in ulcerative colitis. *World Journal of Gastroenterology*, *24*(47), 5322–5330. https://doi.org/10.3748/wjg.v24.i47.5322

Boycott, K. M., Flavelle, S., Bureau, A., Glass, H. C., Fujiwara, T. M., Wirrell, E., Davey, K., Chudley, A. E., Scott, J. N., McLeod, D. R., & Parboosingh, J. S. (2005). Homozygous deletion of the very low density lipoprotein receptor gene causes autosomal recessive cerebellar hypoplasia with cerebral gyral simplification. *American Journal of Human Genetics*, *77*(3), 477–483. https://doi.org/10.1086/444400

Chen, G., Zhang, X., Lin, H., Huang, G., Chen, Y., & Cui, L. (2017). Tanshinol alleviates osteoporosis and myopathy in glucocorticoid-treated rats. *Planta Medica*, *83*(16), 1264–1273. https://doi.org/10.1055/s-0043-108761

Franzosa, E. A., Sirota-Madi, A., Avila-Pacheco, J., Fornelos, N., Haiser, H. J., Reinker, S., Vatanen, T., Hall, A. B., Mallick, H., McIver, L. J., Sauk, J. S., Wilson, R. G., Stevens, B. W., Scott, J. M., Pierce, K., Deik, A. A., Bullock, K., Imhann, F., Porter, J. A., … Xavier, R. J. (2019). Gut microbiome structure and metabolic activity in inflammatory bowel disease. *Nature Microbiology*, *4*(2), 293–305. https://doi.org/10.1038/s41564-018-0306-4

Gao, H., Huang, L., Ding, F., Yang, K., Feng, Y., Tang, H., Xu, Q. M., Feng, J., & Yang, S. (2018). Simultaneous purification of dihydrotanshinone, tanshinone I, cryptotanshinone, and tanshinone IIA from salvia miltiorrhiza and their anti-inflammatory activities investigation. *Scientific Reports*, *8*(1), 8460. https://doi.org/10.1038/s41598-018-26828-0

Guo, Y., Wu, X., Wu, Q., Lu, Y., Shi, J., & Chen, X. (2018). Dihydrotanshinone I, a natural product, ameliorates DSS-induced experimental ulcerative colitis in mice. *Toxicology and Applied Pharmacology*, *344*, 35–45. https://doi.org/10.1016/j.taap.2018.02.018

Gupta, R. A., Motiwala, M. N., Mahajan, U. N., & Sabre, S. G. (2018). Protective effect of *Sesbania grandiflora* on acetic acid induced ulcerative colitis in mice by inhibition of TNF-α and IL-6. *Journal of Ethnopharmacology*, *219*, 222–232. https://doi.org/10.1016/j.jep.2018.02.043

Kim, B. K., Yoo, H. I., Lee, A. R., Choi, K., & Yoon, S. K. (2017). Decreased expression of VLDLR is inversely correlated with miR-200c in human colorectal cancer. *Molecular Carcinogenesis*, *56*(6), 1620–1629. https://doi.org/10.1002/mc.22618

Liu, J., Yang, C. F., Lee, B. L., Shen, H. M., Ang, S. G., & Ong, C. N. (1999). Effect of salvia miltiorrhiza on aflatoxin B1-induced oxidative stress in cultured rat hepatocytes. *Free Radical Research*, *31*(6), 559–568. https://doi.org/10.1080/10715769900301131

Livak, K. J., & Schmittgen, T. D. (2001). Analysis of relative gene expression data using real-time quantitative PCR and the 2(-Delta Delta C [T]) method. *Methods*, *25*(4), 402–408. https://doi.org/10.1006/meth.2001.1262

Luo, S., Deng, X., Liu, Q., Pan, Z., Zhao, Z., Zhou, L., & Luo, X. (2018). Emodin ameliorates ulcerative colitis by the flagellin-TLR5 dependent pathway in mice. *International Immunopharmacology*, *59*, 269–275. https://doi.org/10.1016/j.intimp.2018.04.010

Luo, S., Wen, R., Wang, Q., Zhao, Z., Nong, F., Fu, Y., Huang, S., Chen, J., Zhou, L., & Luo, X. (2019). Rhubarb Peony decoction ameliorates ulcerative colitis in mice by regulating gut microbiota to restoring Th17/Treg balance. *Journal of Ethnopharmacology*, *231*, 39–49. https://doi.org/10.1016/j.jep.2018.08.033

Moon, K., & Cha, J. (2020). Enhancement of antioxidant and antibacterial activities of salvia miltiorrhiza roots fermented with aspergillus oryzae. *Food*, *9*(1), 34. https://doi.org/10.3390/foods9010034

Nunes, N. S., Chandran, P., Sundby, M., Visioli, F., da Costa Gonçalves, F., Burks, S. R., Paz, A. H., & Frank, J. A. (2019). Therapeutic ultrasound attenuates DSS-induced colitis through the cholinergic anti-inflammatory pathway. *eBioMedicine*, *45*, 495–510. https://doi.org/10.1016/j.ebiom.2019.06.033

Pillai, N., Dusheiko, M., Maillard, M. H., Rogler, G., Brüngger, B., Bähler, C., & Pittet, V. E. H. (2019). The evolution of health care utilisation and costs for inflammatory bowel disease over ten years. *Journal of Crohn's & Colitis*, *13*(6), 744–754. https://doi.org/10.1093/ecco-jcc/jjz003

Piodi, L. P., Ulivieri, F. M., Cermesoni, L., & Cesana, B. M. (2004). Long-term intermittent treatment with low-dose 5-aminosalicylic enemas is efficacious for remission maintenance in ulcerative colitis. *Scandinavian Journal of Gastroenterology*, *39*(2), 154–157. https://doi.org/10.1080/00365520310008133

Qiao, C., Yang, L., Wan, J., Liu, X., Pang, C., You, W., & Zhao, G. (2019). Long noncoding RNA ANRIL contributes to the development of ulcerative colitis by miR-323b-5p/TLR4/MyD88/NF-κB pathway. *Biochemical and Biophysical Research Communications*, *508*(1), 217–224. https://doi.org/10.1016/j.bbrc.2018.11.100

Seidelin, J. B., & Nielsen, O. H. (2006). Expression profiling of apoptosis-related genes in enterocytes isolated from patients with ulcerative colitis. *APMIS*, *114*(7–8), 508–517. https://doi.org/10.1111/j.1600-0463.2006.apm_116.x

Seyedian, S. S., Nokhostin, F., & Malamir, M. D. (2019). A review of the diagnosis, prevention, and treatment methods of inflammatory bowel disease. *The Journal of Medicine*, *12*(2), 113–122. https://doi.org/10.25122/jml-2018-0075

Tan, L. L., Liu, L. M., Zhang, X. C., & Piao, C. H. (2018). The effect of miR-17-5p on vascular lesion and expression of VLDLR in atherosclerotic mice. *Sichuan Da Xue Xue Bao. Yi Xue Ban*, *49*(4), 507–511.

Tatiya-Aphiradee, N., Chatuphonprasert, W., & Jarukamjorn, K. (2018). Immune response and inflammatory pathway of ulcerative colitis. *Journal of Basic and Clinical Physiology and Pharmacology*, *30*(1), 1–10. https://doi.org/10.1515/jbcpp-2018-0036

Vijayan, V., Pradhan, P., Braud, L., Fuchs, H. R., Gueler, F., Motterlini, R., Foresti, R., & Immenschuh, S. (2019). Human and murine macrophages exhibit differential metabolic responses to lipopolysaccharide—A

divergent role for glycolysis. *Redox Biology*, *22*, 101147. https://doi.org/10.1016/j.redox.2019.101147

Walana, W., Ye, Y., Li, M., Wang, J., Wang, B., Cheng, J. W., Gordon, J. R., & Li, F. (2018). IL-8 antagonist, CXCL8(3-72)K11R/G31P coupled with probiotic exhibit variably enhanced therapeutic potential in ameliorating ulcerative colitis. *Biomedicine & Pharmacotherapy*, *103*, 253–261. https://doi.org/10.1016/j.biopha.2018.04.008

Wang, Y., & Zhang, D. (2020). Tanshinol inhibits growth of malignant melanoma cells via regulating miR-1207-5p/CHPF pathway. *Archives of Dermatological Research*, *312*(5), 373–383. https://doi.org/10.1007/s00403-019-01992-z

Xing, B., Yang, D., Guo, W., Liang, Z., Yan, X., Zhu, Y., & Liu, Y. (2014). Ag+ as a more effective elicitor for production of tanshinones than phenolic acids in salvia miltiorrhiza hairy roots. *Molecules*, *20*(1), 309–324. https://doi.org/10.3390/molecules20010309

Yan, Y. X., Shao, M. J., Qi, Q., Xu, Y. S., Yang, X. Q., Zhu, F. H., He, S. J., He, P. L., Feng, C. L., Wu, Y. W., Li, H., Tang, W., & Zuo, J. P. (2018). Artemisinin analogue SM934 ameliorates DSS-induced mouse ulcerative colitis via suppressing neutrophils and macrophages. *Acta Pharmacologica Sinica*, *39*(10), 1633–1644. https://doi.org/10.1038/aps.2017.185

Yang, Y., Su, Y., Wang, D., Chen, Y., Liu, Y., Luo, S., Wu, T., & Cui, L. (2016). Tanshinol rescues the impaired bone formation elicited by glucocorticoid involved in KLF15 pathway. *Oxidative Medicine and Cellular Longevity*, *2016*, 1092746. https://doi.org/10.1155/2016/1092746

Zhang, W. J., Wang, S., Kang, C. Z., Lv, C. G., Zhou, L., Huang, L. Q., & Guo, L. P. (2020). Pharmacodynamic material basis of traditional Chinese medicine based on biomacromolecules: A review. *Plant Methods*, *16*, 26. https://doi.org/10.1186/s13007-020-00571-y

Zhu, P., Liu, Z., Zhou, J., & Chen, Y. (2019). Tanshinol inhibits the growth, migration and invasion of hepatocellular carcinoma cells via regulating the PI3K-AKT signaling pathway. *Oncotargets and Therapy*, *12*, 87–99. https://doi.org/10.2147/ott.S185997

SUPPORTING INFORMATION

Additional supporting information may be found online in the Supporting Information section at the end of this article.